Electronic Supporting Information

Irving-Williams series guided construction of a stable core–shell MnHCF@CuHCF cathode

Shumin Sun,*[a] Haibo Lei,[a] Yunpeng Ma,[a] Yonghui Zhang,[a] Xia Cao*[a,b] and Peiyuan Wang*[a,c]

[a] *College of Material and Chemical Engineering, Zhengzhou University of Light Industry, Zhengzhou 450001, P. R. China. E-mail: smsun@zzuli.edu.cn*

[b] *Collaborative Innovation Center of Environmental Pollution Control and Ecological Restoration of Henan Province, Zhengzhou 450001, China. E-mail: 2020003@zzuli.edu.cn*

[b] *Henan Provincial Key Laboratory of Surface and Interface Science, Zhengzhou University of Light Industry, Zhengzhou 450001, P. R. China. E-mail: peiyuanwang@zzuli.edu.cn*

[a] *College of Material and Chemical Engineering, Zhengzhou University of Light Industry, Zhengzhou 450001, P. R. China. E-mail: smsun@zzuli.edu.cn*

[b] *Collaborative Innovation Center of Environmental Pollution Control and Ecological Restoration of Henan Province, Zhengzhou 450001, China. E-mail: 2020003@zzuli.edu.cn*

[c] *Henan Provincial Key Laboratory of Surface and Interface Science, Zhengzhou University of Light Industry, Zhengzhou 450001, P. R. China. E-mail: peiyuanwang@zzuli.edu.cn*

Synthesis of Prussian blue analogue

MnHCF@CuHCF was synthesized via a co-precipitation method. The typical synthesis procedure is as follows: 5 mmol of $Na_4Fe(CN)_6 \cdot 10H_2O$ was dissolved in 100 mL of deionized water (DI) to form Solution A. Separately, 1 mmol of $CuSO_4 \cdot 5H_2O$, 4 mmol of $MnSO_4 \cdot H_2O$, and 25 mmol of sodium citrate were dissolved in another 100 mL of DI water to form Solution B. Using a peristaltic pump, both solutions were then simultaneously added dropwise at a flow rate of 10 mL/h into a three-necked flask containing 200 mL of DI water. During the addition, the mixture was continuously stirred under an argon atmosphere for 12 h. After the reaction, the mixture was aged for 12 h without stirring, and the precipitate was collected by centrifugation. The obtained solid was washed several times with deionized water and ethanol, and then dried in a vacuum oven at 120 °C for 12 h. The final product was denoted as MnHCF@CuHCF.

For comparison, MnHCF and CuHCF were prepared using similar procedures. In the case of MnHCF, Solution B contained 5 mmol of $MnSO_4 \cdot H_2O$ and 25 mmol of sodium citrate in 100 mL of DI water, while for CuHCF, Solution B contained 5 mmol of $CuSO_4 \cdot 5H_2O$ and 25 mmol of sodium citrate in 100 mL of DI water. The remaining steps were identical to those described above.

Material characterization

The as-synthesized samples were characterized to elucidate their physicochemical properties. Their morphologies and microstructures were examined using scanning electron microscopy (SEM, ZEISS Sigma 360) and transmission electron microscopy (TEM, FEI Tecnai G2 F20). The crystalline phase was identified by X-ray diffraction (XRD) on a Bruker D8 Advance instrument with Cu Kα radiation (λ = 1.54056 Å), scanning a 2θ range from 5° to 80°. The XRD data were analyzed by Rietveld refinement with GSAS software.[1] X-ray photoelectron spectroscopy (XPS, Thermo Fisher Scientific) was employed to analyze the surface chemical composition and the valence states of Mn, Fe, and Cu. Raman spectra were acquired with a confocal laser micro-Raman spectrometer (HORIBA, Lab RAM HR Evolution). Finally, the elemental contents of Mn, Fe, Cu, and Na were quantified by inductively coupled

plasma mass spectrometry (ICP-MS, ELAN 9000).

Reference

1. Larson, A. C. & Dreele, R. B. V. General structure analysis system (GSAS) (Report LAUR 86-748, Los Alamos National Laboratory, 2004).

Electrochemical measurements

The electrochemical properties of the obtained MnHCF, CuHCF, and MnHCF@CuHCF materials were tested by assembling CR2032 coin cells in an argon-protected glovebox (MIKROUNA, Model Super 1220/750/900, H_2O < 0.1 ppm, O_2 < 0.1 ppm). The cell assembly parameters are as follows: MnHCF, CuHCF, and MnHCF@CuHCF were used as the working electrodes, metallic sodium as the counter electrode, the electrolyte was a 1.0 mol/L sodium perchlorate ($NaClO_4$) solution in a mixture of ethylene carbonate (EC), dimethyl carbonate (DMC), and ethyl methyl carbonate (EMC) (volume ratio 1:1:1) with the addition of 2 vol.% fluoroethylene carbonate (FEC), and Whatman glass fiber was employed as the separator. The preparation process of the working electrodes is as follows: First, the MnHCF, CuHCF, or MnHCF@CuHCF material, Ketjen black (conductive agent), and polyvinylidene fluoride (PVDF, binder) were mixed at a mass ratio of 7:2:1, and dispersed in N-methyl-2-pyrrolidone (NMP) to form a homogeneous slurry. Subsequently, the slurry was uniformly coated on aluminum foil and dried in a vacuum oven at 120℃ for 12 h. Finally, the aluminum foil coated with MnHCF, CuHCF, or MnHCF@CuHCF was punched into 14 mm-diameter disks to obtain the working electrodes, with the active material loading mass of approximately 1 mg. For electrochemical measurements, galvanostatic charge-discharge testing, cyclic voltammetry (CV), and electrochemical impedance spectroscopy (EIS) were performed using a Land battery testing system (China, Model CT4008TNn-5V10mA-164) and an electrochemical workstation (China, Model CHI660e), respectively. The cells were galvanostatically charged and discharged between 2.0 and 4.0 V at various current densities. The capacity was calculated based on the mass of the active material in the electrode, excluding the mass of the conductive carbon (Ketjen black).

Galvanostatic intermittent titration (GITT) measurement was used to evaluate the Na^+ diffusion coefficient (D) of the PB-B and PB-H. D can be calculated by using Fick's second law as follows:

$$D = \frac{4}{\pi\tau}\left(\frac{V_M m_B}{S M_B}\right)^2 \left(\frac{\Delta E_s}{\Delta E_\tau}\right)^2$$

where V_M, m_B, M_B, and S are molar volume, mass, molar mass, and electrode area, respectively. τ is the pulse time (s). ΔE_s and ΔE_τ are the differences of voltage and time, respectively.

Table S1. Crystallographic parameters of CuHCF obtained from XRD Rietveld refinement.

CuHCF, Cubic, space group Fm-3m, a = b = c = 10.054275 Å, α = β = γ = 90°, V = 1016.371 Å3, weighted profile R-factor, Rwp=8.76 %.					
Atom	X	Y	Z	Site	Occ
Fe1	0.00000	0.00000	0.00000	4a	1.0000
Cu2	0.00000	0.00000	0.50000	4b	1.0000
Na3	0.25000	0.25000	0.25000	8c	1.0000
C4	0.00000	0.00000	0.188400	24e	1.0000
N5	0.00000	0.00000	0.300400	24e	1.0000

Table S2. Crystallographic parameters of MnHCF obtained from XRD Rietveld refinement.

MnHCF, Cubic, space group Fm-3m, a = b = c = 10.537680 Å, α = β = γ = 90°, V = 1170.132 Å3, weighted profile R-factor, Rwp=27.6 %.					
Atom	X	Y	Z	Site	Occ
Fe1	0.00000	0.00000	0.00000	4a	1.0000
Mn2	0.50000	0.00000	0.00000	4b	1.0000
Na3	0.25000	0.25000	0.25000	32c	1.0000
C4	0.19710	0.17530	0.00000	24e	1.0000
N5	0.29110	0.00000	0.00000	24e	1.0000

Table S3. Crystallographic parameters of MnHCF@CuHCF obtained from XRD Rietveld refinement.

MnHCF@CuHCF CuHCF, Cubic, space group Fm-3m, a = b = c = 10.055225 Å, α = β = γ = 90°, V = 1016.371 Å3, weighted profile R-factor, Rwp=12.7 %.					
Atom	X	Y	Z	Site	Occ
Fe1	0.00000	0.00000	0.00000	4a	1.0000
Cu2	0.00000	0.00000	0.50000	4b	1.0000
Na3	0.25000	0.25000	0.25000	8c	1.0000
C4	0.00000	0.00000	0.18840	24e	1.0000
N5	0.00000	0.00000	0.30040	24e	1.0000

MnHCF@CuHCF MnHCF, Cubic, space group Fm-3m, a = b = c = 10.352860 Å, α = β = γ = 90°, V = 1170.132 Å3, weighted profile R-factor, Rwp=12.7 %.					
Atom	X	Y	Z	Site	Occ
Fe1	0.00000	0.00000	0.00000	4a	1.0000
Mn2	0.50000	0.00000	0.00000	4b	1.0000
Na3	0.25000	0.25000	0.25000	8c	1.0000
C4	0.17530	0.00000	0.00000	24e	1.0000
N5	0.29110	0.00000	0.00000	24e	1.0000

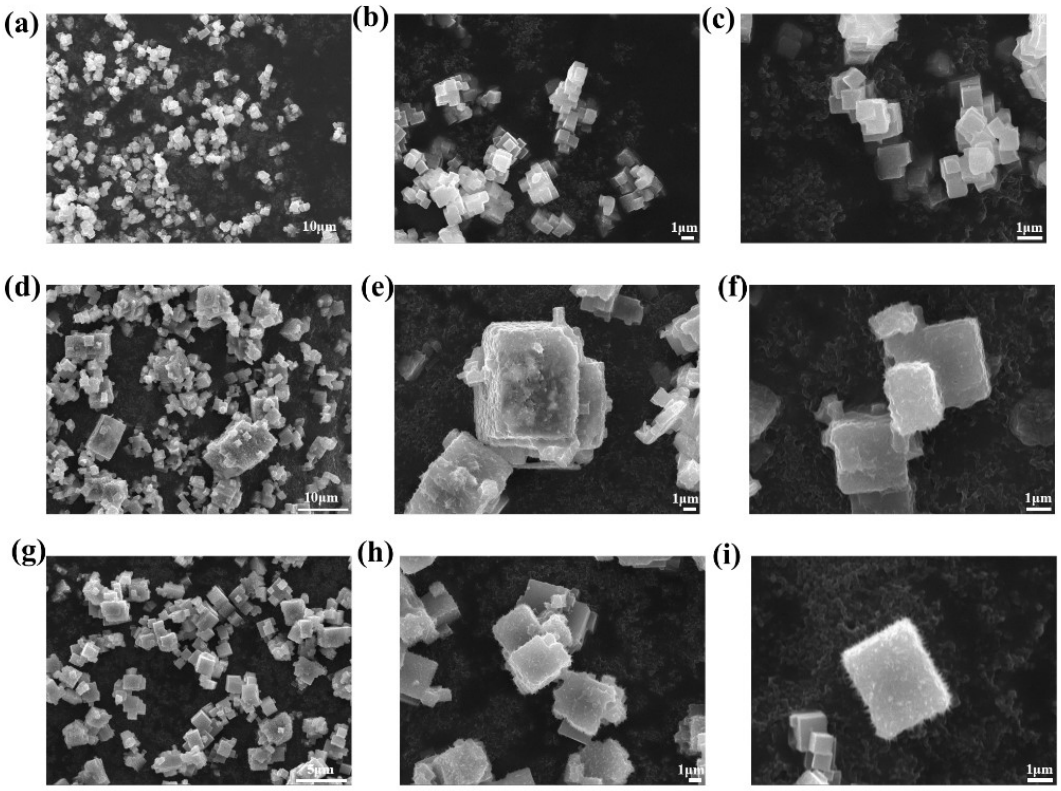

Fig. S1 SEM image of CuHCF (a-c), MnHCF (d-f) and MnHCF@CuHCF (g-i).

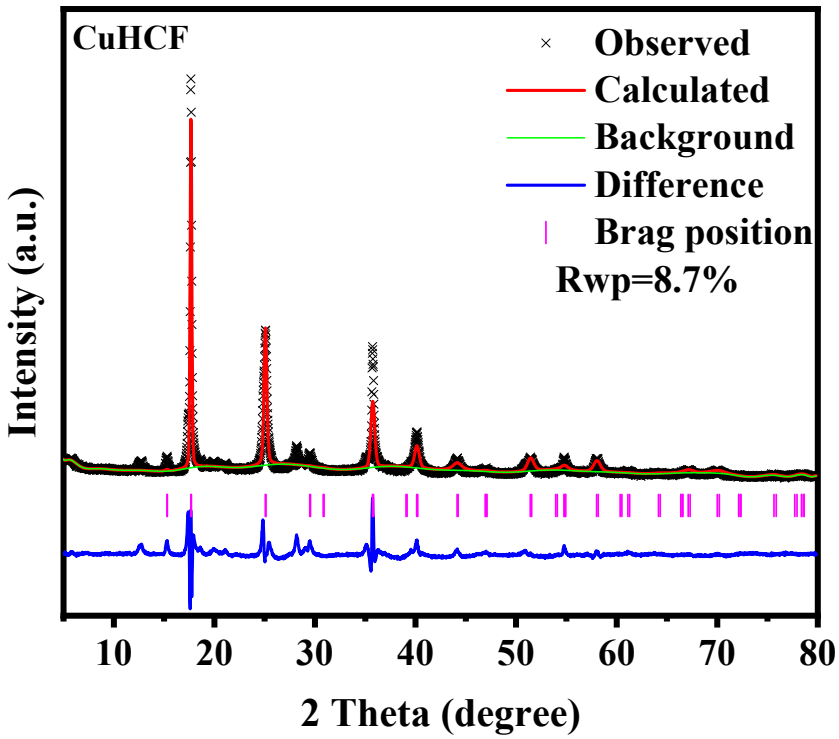

Fig. S2 The XRD patterns of CuHCF

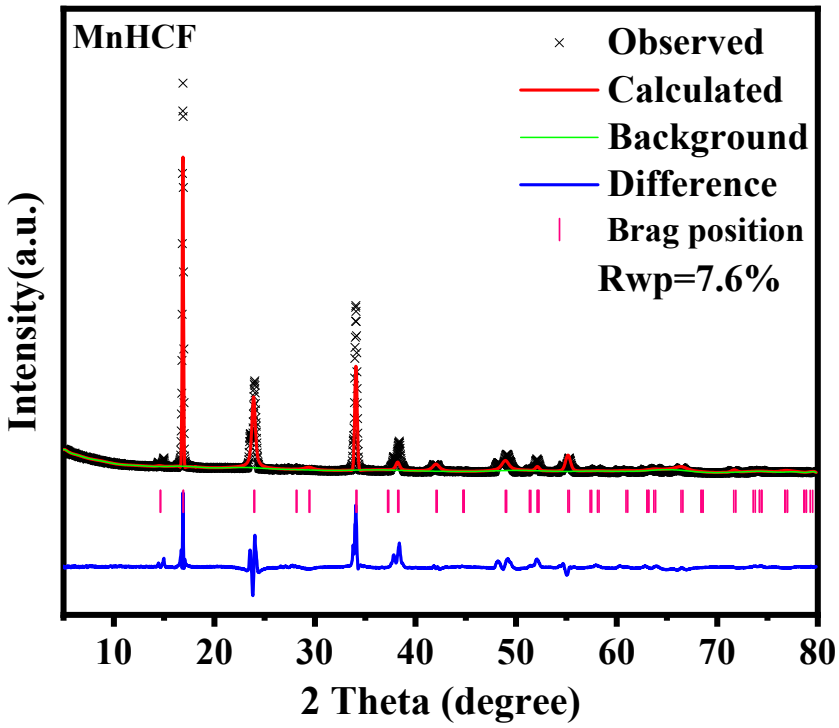

Fig. S3 The XRD patterns of MnHCF

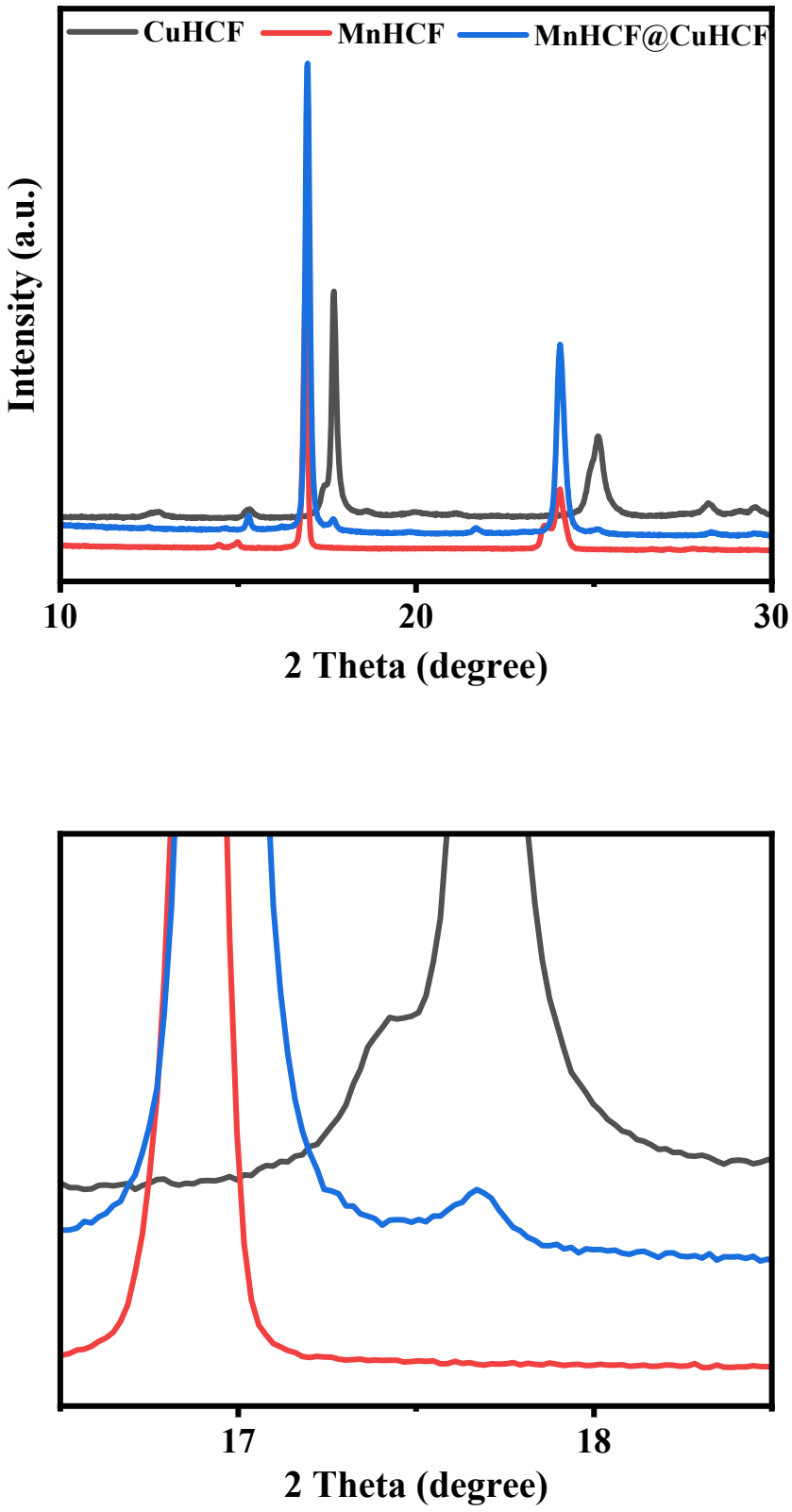

Fig. S4 The XRD patterns of CuHCF, MnHCF and MnHCF@CuHCF

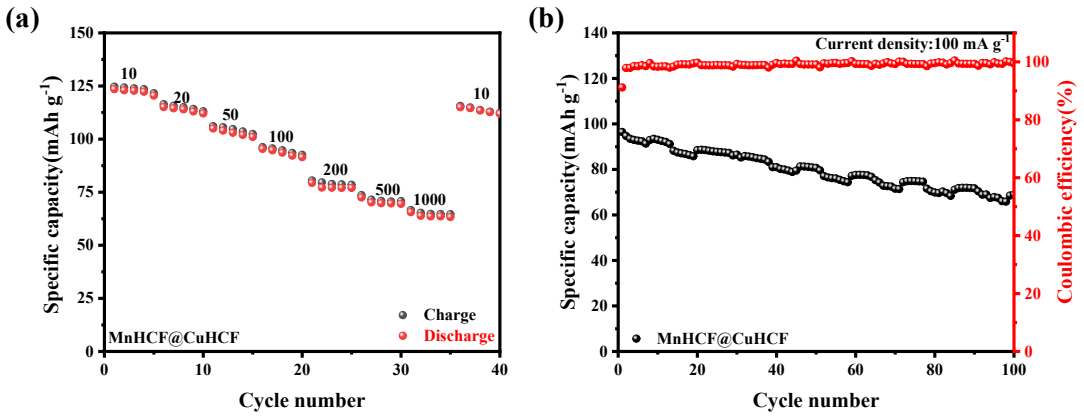

Fig. S5 The rate capability (a) and cycling performance at a current density of 100 mA g^{-1} (b) for MnHCF@CuHCF.

The selection of this specific electrolyte system was based on several key considerations. First, $NaClO_4$ offers high solubility and ionic conductivity in carbonate-based solvents, which facilitates efficient sodium-ion transport. Second, the ternary solvent mixture of EC, DMC, and EMC (1:1:1 by volume) combines the high dielectric constant of EC with the low viscosity of linear carbonates (DMC and EMC), ensuring stable electrochemical performance across a wide temperature range. Furthermore, the addition of 2 vol.% FEC promotes the formation of a robust and stable solid electrolyte interphase (SEI) on the electrode surface, thereby enhancing cycling stability. (Acta Phys. -Chim. Sin. 2009,25,201-206.)

For comparison, we also evaluated a baseline electrolyte composed of 1.0 M $NaClO_4$ in EC/DMC (1:1 by volume). The corresponding charge–discharge curves are presented in the figure below. The results indicate that the EC/DMC/EMC-based electrolyte delivers superior long-term cycling and rate performance, which can be attributed to the incorporation of EMC further optimizing solvent viscosity and SEI-forming characteristics. Future work will involve systematic optimization of electrolyte composition in relation to electrode compatibility.

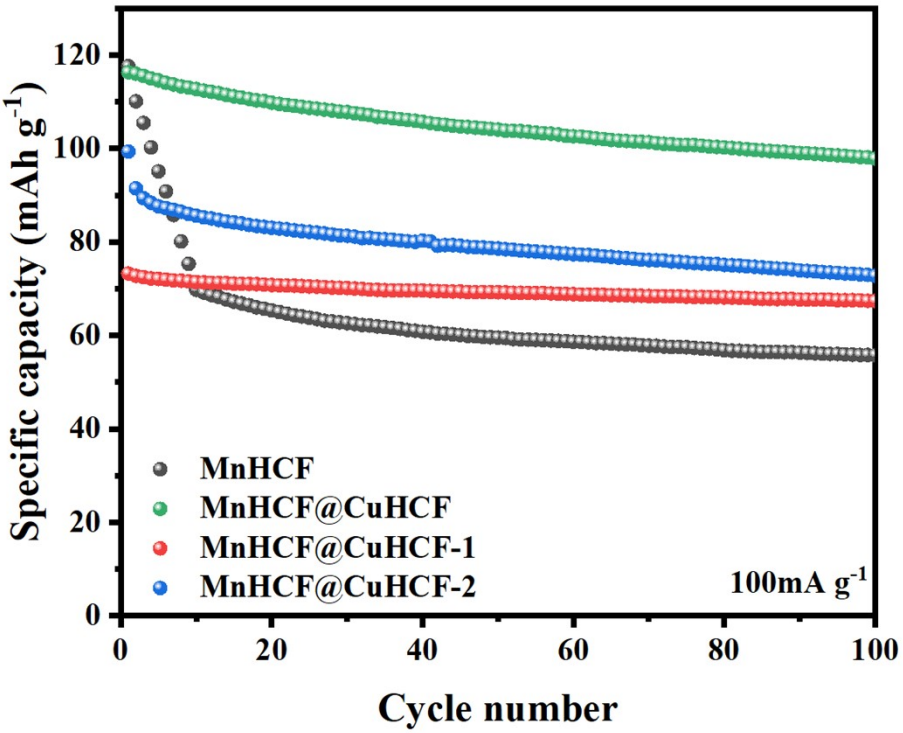

Fig. S6 Cycling performances of MnHCF, MnHCF@CuHCF, MnHCF@CuHCF-1 and MnHCF@CuHCF-2 at a current density of 100 mA g^{-1}.

A series of composite materials by changing the Mn: Cu molar ratio in the initial raw materials, specifically including MnHCF@CuHCF (Mn: Cu = 4:1), MnHCF@CuHCF-1 (Mn:Cu = 1:1), and MnHCF@CuHCF-2 (Mn:Cu = 1:4). The results indicate that while MnHCF materials without CuHCF coating deliver excellent initial specific capacity, their cycling performance requires further improvement. With the introduction of a small amount of CuHCF coating, the MnHCF@CuHCF material shows a slight decrease in specific capacity, but its cycling stability is significantly enhanced. On the other hand, MnHCF@CuHCF-1 and MnHCF@CuHCF-2, with thicker CuHCF coatings, demonstrate superior cycling stability but exhibit a significant reduction in specific capacity. Overall, MnHCF@CuHCF achieves an optimal balance between specific capacity and cycling stability, exhibiting outstanding overall performance.

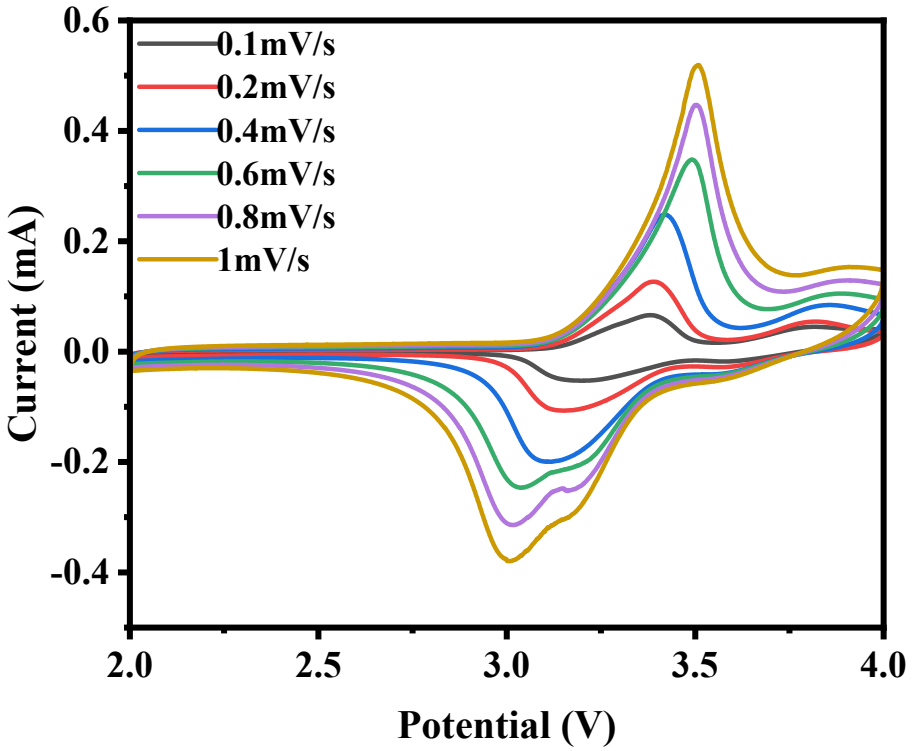

Fig. S7 CV of MnHCF@CuHCF at scan rates ranging from 0.1 to 1.0 $mV \cdot s^{-1}$